Tumor-Targeting Potential of Radioiodinated Iododeoxyuridine in Bladder Cancer

Annick D. Van den Abbeele, Ronald F. Tutrone, Robert M. Berman, Janina Baranowska-Kortylewicz, Paul D. Barclay, Jerome P. Richie, S. James Adelstein and Amin I. Kassis

Department of Radiology (Nuclear Medicine) and Division of Urology, Harvard Medical School, Boston, Massachusetts

Since bladder cancer arises in the superficial lining of the urothelium, it is a likely candidate for site-directed administration of 5-iodo-2'-deoxyuridine radiolabeled with the Auger electron emitter ^{123}I or ^{125}I (*IUdR). **Methods:** We instilled *IUdR for 2 hr directly within the bladder lumen of rats bearing N-methyl-N-nitrosourea (NMU)-induced bladder cancer and conducted scintigraphic, biodistribution and autoradiography (ARG) studies 48 hr and 1 wk later. Control animals were not subjected to the carcinogen but were instilled with *IUdR. **Results:** Two groups of animals were identified after instillation of MNU: Group A consisted of rats with hyperplasia and Group B of rats with papillary carcinoma (stages Ta and T1). Scintigraphic detection of carcinomas was achieved with high sensitivity and specificity, and increased tumor-to-normal tissue ratios were obtained in both groups. Moreover, ARG demonstrated that (1) the uptake of *IUdR was observed in the hyperplastic and carcinomatous urothelium but not in the normal urothelium; (2) uptake was detected at a very early stage of tumor development (hyperplasia stage); (3) *IUdR was able to penetrate deep within the bladder wall; and (4) other normal dividing tissues, such as the bone marrow, the small intestine and the large intestine, were free of silver grains (i.e., no DNA-incorporated *IUdR). **Conclusion:** Since this carrier of Auger electron emitters has antineoplastic effects ([^{123}I]IUdR and [^{125}I]IUdR) in addition to its scintigraphic potential ([^{123}I]IUdR and [^{131}I]IUdR), it holds promise for therapy and early diagnosis of bladder cancer.

Key Words: Auger electron emitters; 5-iodo-2'-deoxyuridine; bladder cancer; radioiodine

J Nucl Med 1996; 37:315–320

Cancer of the bladder is the fifth leading cause of cancer mortality in the United States (*1*); an estimated 52,300 new cases of bladder cancer occurred in 1993 (*2*). This is largely a disease of the elderly, with a peak prevalence between 60 and 70 yr of age (*2,3*). Most patients (74%) present with superficial localized tumors that arise from the transitional epithelium, about 90% of which are transitional cell carcinomas (*1,2,4*). Cytologic examination and cystoscopy play a critical role in the early diagnosis and evaluation of bladder cancer (*1*) as well as in its follow-up. Although endoscopic treatment is usually feasible in cases of superficial tumors, the major problem stems from the high frequency of recurrence (up to 75%) within 6 to 12 mo after initial treatment, thus requiring serial re-evaluation and close follow-up (*1,4*). Intravesical chemotherapy with thiotepa, doxorubicin, mitomycin C or bacillus Calmette-Guerin has been shown to lower the recurrence rate and extend the disease-free interval (*1*). Since patients with positive cytology after endoscopic treatment may not present macroscopic changes for some time (*5,6*), they are at high risk for tumor invasion and subsequent distant metastases (*1*). There is a need for a better understanding of the intrinsic biologic behavior of each individual tumor to identify increased risk for progression/recurrence and to allow tailoring of the therapeutic regimen (*3*).

The radionuclides ^{123}I and ^{125}I, both commercially available, are prolific emitters of Auger electrons. The radiotherapeutic effectiveness of these radionuclides following DNA incorporation through the thymidine analog 5-iodo-2'-deoxyuridine ([^{123}I]IUdR and [^{125}I]IUdR) has already been demonstrated in vivo in an experimental murine ascites tumor model of ovarian origin after intraperitoneal injection (*7–9*), in a murine intracerebral 9L solid gliosarcoma tumor after intracranial injection (*10*) and in a murine meningeal carcinomatosis model after intrathecal infusion (*11*). These findings suggest that IUdR radiolabeled with an Auger electron emitter (*IUdR) may be an efficient therapeutic agent for the treatment of cancers that are accessible to direct intralesional or intracavitary delivery of the radiopharmaceutical. In addition, when IUdR is radiolabeled with the gamma-ray-emitting ^{123}I and administered locoregionally into animals bearing intraperitoneal or intracranial tumors, this radiopharmaceutical has proved to be a very sensitive agent for the detection of experimental tumors by scintigraphy (*9,12*).

The rationale behind the potential use of *IUdR in the diagnosis and therapy of bladder cancer rests on the following arguments. Since this cancer arises in the superficial lining of the bladder wall which is accessible via catheterization, and neoplastic cells are actively dividing while normal urothelium is essentially quiescent [for example, the labeling index using ^{3}HTdR for papillary and sessile carcinoma 11.16%, range 0.70%–32.5%, while that for normal urothelium 0.13%, range 0.00%–0.40% (*13*)], we hypothesized that the intravesical delivery of the thymidine analog IUdR would result in its incorporation into the proliferating cells, but not normal tissue. Since IUdR can be labeled with a gamma-emitting radionuclide, the visualization of these tumors via scintigraphy would be possible. Finally, autoradiography would demonstrate the DNA incorporation and targeting specificity and, therefore, the therapeutic potential of *IUdR.

To test our hypothesis, we instilled *IUdR directly within the bladder lumen of rats bearing chemically-induced bladder cancer and conducted scintigraphic, biodistribution, and autoradiographic studies 48 hr and 1 wk later. Control animals were not subjected to the carcinogen but were injected by the same route with identical amounts of *IUdR.

MATERIALS AND METHODS

Tumor Model

The carcinogen N-methyl-N-nitrosourea (MNU), which is known to induce transitional cell carcinoma of the bladder, was instilled directly into the bladder lumen of 4–5-wk-old female Fisher 344 rats (20 animals) by bladder catheterization using a 22-gauge angiocatheter (1.5 mg/0.15 ml saline intravesically, every other week for a total of four doses) (*14*). Drinking water was supplemented with a combination of trimethoprim-sulfamethoxasole, neomycin sulfate and polymixin B. Twelve to sixteen wk after

Received Dec. 16, 1994; revision accepted Jul. 29, 1995.

For correspondence or reprints contact: Amin I. Kassis, PhD, Shields Warren Radiation Laboratory, 50 Binney St., Boston, MA 02115.

the last MNU infusion, the bladder was catheterized and emptied and a mixture of [^{125}I]IUdR and [^{131}I]IUdR (~6–11 MBq [^{125}I]IUdR [~170–300 μCi] and ~11 MBq [^{131}I]IUdR [~300 μCi]) was administered through the catheter in a 100- or 200-μl volume and left in place for 2 hr. The bladder contents were then withdrawn and the bladder was rinsed several times with normal saline (5 × 1-ml wash). Nontumor-bearing control rats (16 animals) were given identical amounts of [^{125}I/^{131}I]IUdR by the same route. The drinking water of all animals was supplemented with potassium iodide (0.1% KI) from 48 to 72 hr prior to the administration of the radiopharmaceutical up to the time of sacrifice at 48 hr (n = 12 tumor-bearing and 12 control) or 1 wk (n = 8 tumor-bearing and 4 controls) after instillation of *IUdR.

Synthesis of 5-[^{131}I/^{125}I]Iodo-2′-deoxyuridine (*IUdR)

Iodine-125 (specific activity 81.4 TBq/mmole) and iodine-131 (specific activity 96.9 GBq/mmole) were purchased from Du Pont NEN Research Products (Boston, MA), and Amersham Corporation, (Arlington Heights, IL), respectively. No-carrier-added [^{125}I/^{131}I]IUdR was synthesized as described previously (*15*) and purified on a C_{18} reverse phase HPLC column. The radiochemical purity of the product was >99% as determined by HPLC.

Scintigraphy

Planar scintigraphic images were obtained with a GE Camstar gamma camera (GE, Milwaukee, WI) 4 hr and 3 and 7 days after instillation of [^{131}I]IUdR (gamma camera equipped with an ME collimator, anterior views, 256 × 256 matrix, 20% window, 5-min acquisition, 2.0 magnification). A 5-min acquisition time was used at the 4-hr time point, and the number of counts for that time period was measured. On Day 3 and Day 7, the same number of counts were acquired. We opted to use [^{131}I]IUdR in these studies because of its longer half-life compared with [^{123}I]IUdR (8 days versus 13.2 hr) which permits imaging at later time points.

Pathology and Biodistribution

Pathology and biodistribution studies were performed 48 hr and 1 wk after instillation of *IUdR. Both control and MNU-treated bladders were rinsed with normal saline and fixed in situ with 10% buffered formaldehyde. To quantitate the in vivo distribution of the radiopharmaceutical (percent injected dose per gram of tissue, %ID/g) and to derive the tumor-to-normal tissue ratios, various organs and tissues of interest—bladder, kidneys, uterus, ovaries, skin, muscle, stomach, small intestine, large intestine, spleen, liver, heart, lungs, bone and thyroid—were excised, rinsed in normal saline, blotted dry, weighed, and their radioactive content was determined in a gamma counter along with that of urine, stomach contents, blood and bone marrow. The small and large intestines were quickly frozen in isopentane and liquid nitrogen. Bone marrow smears were fixed in 100% methanol. The bladders were then embedded in paraffin, sectioned, stained with hematoxylin and eosin, and examined for pathology.

Autoradiography (ARG)

The actual specificity of targeting of DNA-incorporated [^{125}I]IUdR was determined by microautoradiography. The distribution of grains was assessed over the entire section and compared with the histopathology findings. The bladder, frozen tissues and bone marrow smears obtained from the biodistribution studies were sectioned (5–7 μm thickness), fixed (except for the bladder sections already fixed in vivo) and processed for ARG.

The tissue sections and bone marrow slides were coated with NTB2 emulsion (Kodak, Rochester, NY) and stored desiccated at 4°C in light-tight boxes. After various times of emulsion exposure (up to 4 mo), the autoradiography slides were developed for 3 min in D-19 developer (Kodak) and fixed for 5 min in D-11 fixer (Kodak). Finally, the tissue sections were washed in distilled water,

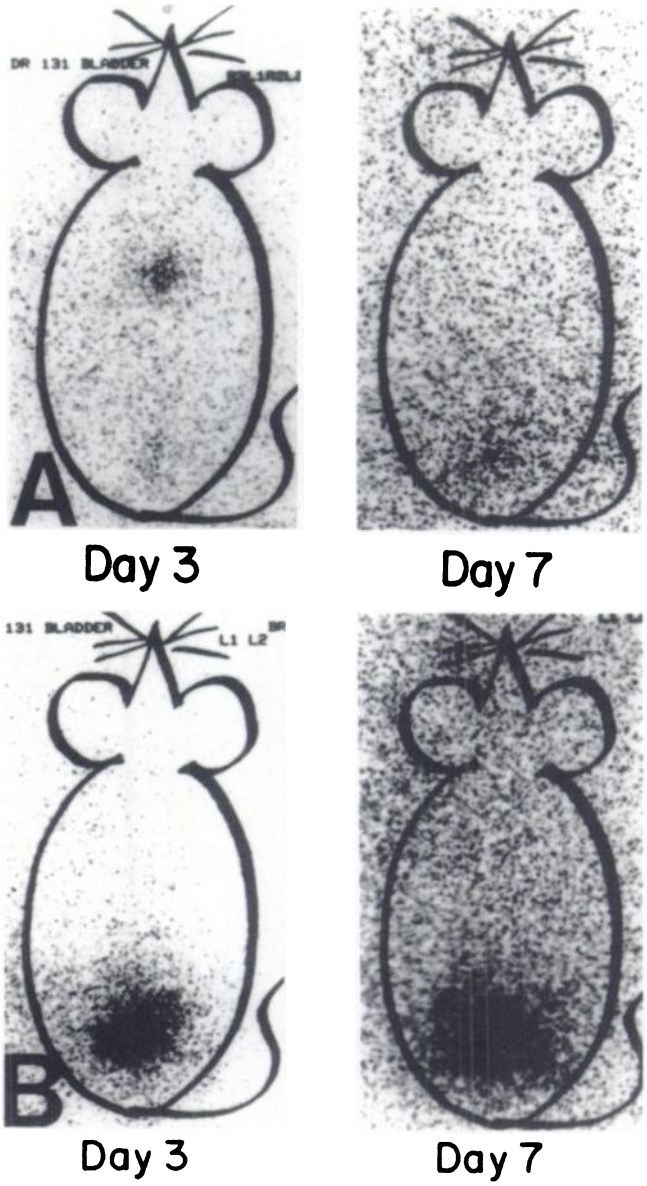

FIGURE 1. Scintigraphic images obtained in normal rats (A) and tumor-bearing rats (B) 3 and 7 days after intravesical administration of [^{131}I]IUdR (BL = bladder).

stained with hematoxylin and eosin, dehydrated, cleared and mounted in Permount. Bone marrow slides were stained with Giemsa stain. All slides were examined under light microscopy.

RESULTS

Scintigraphy

Planar scintigraphic images (Fig. 1), obtained over a 1-wk period after intravesical administration of [^{131}I]IUdR, demonstrated the virtual absence of activity in normal animals on the third day, while the only visible area of activity in the tumor-bearing animals was over the region of the bladder. These types of images persisted on the seventh day after injection.

Pathology and Biodistribution

Examination of the animal bladders subjected to the carcinogen MNU revealed two stages of the disease: one group of animals with hyperplastic changes (Group A, n = 7) and one with papillary carcinomatous changes of the urothelium (Group B, n = 10). Both groups had superficial disease limited to the mucosa and the submucosa (stages Ta [n = 8] and T1 [n = 2]

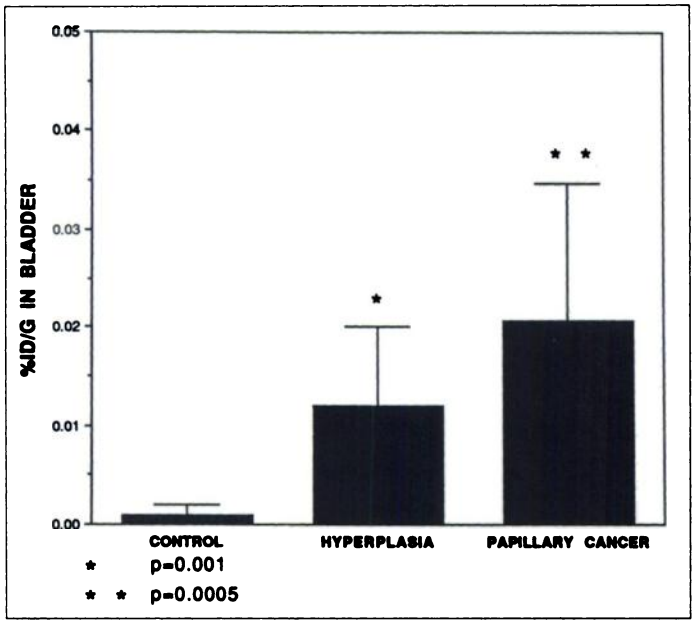

FIGURE 2. Percent injected dose per gram of bladder (mean ± s.d.) 48 hr after intravesical administration of [^{125}I]IUdR as function of pathology (t-test: *p = 0.001; **p = 0.0005).

of the American Joint Committee [AJC] system). Several animals also presented additional squamous metaplasia. Animals with no evidence of tumor (n = 3) were excluded, as were those with active infection (n = 2), because uptake of *IUdR by proliferating bacteria spuriously elevated the radioactive content of the bladder. These animals also frequently developed stones and calcifying and/or ossifying fibrosis of the bladder wall.

The 48-hr biodistribution data (Fig. 2) indicated a significant difference in the %ID/g in the bladder of tumor-bearing animals (hyperplasia [Group A]: p = 0.001; papillary carcinoma [Group B]: p = 0.0005) compared to the control group. The %ID/g was 0.012 ± 0.008 for Group A and 0.021 ± 0.014 for Group B versus 0.0009 ± 0.001 for the control.

At the time of the biodistribution studies, it was noted that all tumor-bearing animals had evidence of bilateral hydronephrosis and megaureters with wide communication between the bladder and the ureters. This complication, which seldom occurs in bladder cancer patients, contributed to the systemic distribution of the radiopharmaceutical (0.02517% ± 0.04070% and 0.0009% ± 0.00097 %ID/g blood at 48 hr and 8 days, respectively). In the control group, on the other hand, most of the intravesical *IUdR solution remained within the bladder and permeation to the systemic circulation was very low (0.00054% ± 0.00046% and 0.0001% ± 0.0 %ID/g blood at 48 hr and 8 days, respectively), limited to normal diffusion and/or effects of possible minimal trauma to the bladder wall secondary to the catheterization procedure. In order to obtain a better assessment of the expectations in humans where the delivery of the radiopharmaceutical would be well controlled and confined to the bladder, we expressed the target-to-nontarget ratios as the quotient of the activity observed in the bladder of the tumor-bearing animals to that of the normal tissues of the control animals. These ratios (Fig. 3) are all above 1 ranging in the hyperplasia group from 2 (bone) to 43 (muscle), the bladder being 12, and in the papillary carcinoma group from 4 (bone) to 93 (muscle), the bladder being 26.

The 1-wk biodistribution data (Fig. 4) indicated a significant difference in the %ID/g in the bladder of animals with hyperplasia (Group A: p = 0.002) but not in the papillary carcinoma

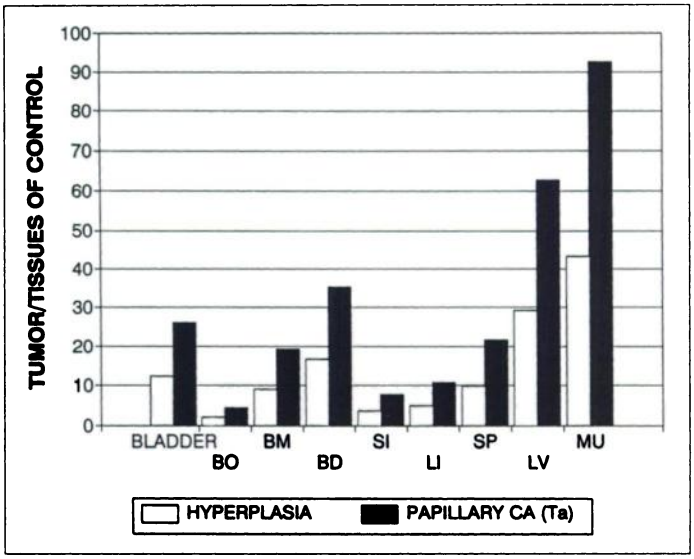

FIGURE 3. Tumor-to-normal tissue ratios 48 hr after intravesical administration of [^{125}I]IUdR (BO = bone, BM = bone marrow, BD = blood, SI = small intestine, LI = large intestine, SP = spleen, LV = liver, MU = muscle).

group (Group B: p = 0.104) compared to the control group. The %ID/g was 0.0011 ± 0.00025 for Group A and 0.0052 ± 0.0048 for Group B versus 0.00013 ± 0.00013 for the control group. This may be due to the wider variation observed within groups at that time and to the fact that, within 1-wk, a significant shedding of the papillary carcinomatous urothelium may have taken place, thereby eliminating a significant portion of cells that had taken up *IUdR. The activity quotient observed in the bladder of Group A to that of the normal tissues of the control animals (Fig. 5) were all above one, ranging from 5 (small intestine) to 26 (liver), the bladder being 12, and in Group B from 29 (small intestine) to 148 (liver), the bladder being 66.

Autoradiography

Autoradiography confirmed the biodistribution data, demonstrating uptake of *IUdR by the tumor at early stages of tumor

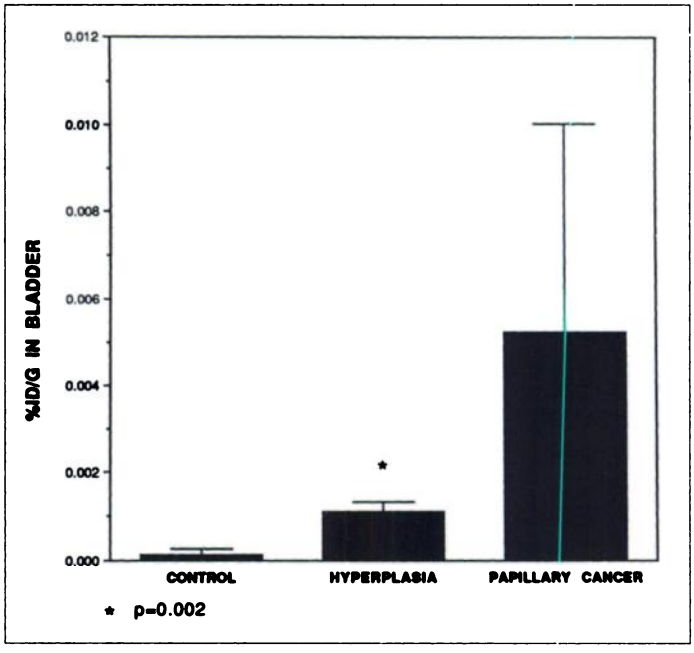

FIGURE 4. Percent injected dose per gram of bladder (mean ± s.d.) 1 wk after intravesical administration of [^{125}I]IUdR as function of pathology (t-test: *p = 0.002).

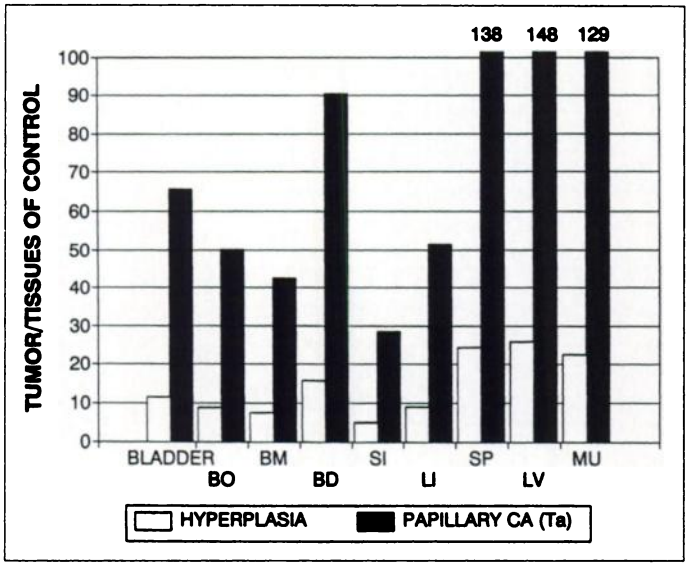

FIGURE 5. Tumor-to-normal tissue ratios 1 week after intravesical administration of [^{125}I]IUdR (BO = bone, BM = bone marrow, BD = blood, SI = small intestine, LI = large intestine, SP = spleen, LV = liver, MU = muscle).

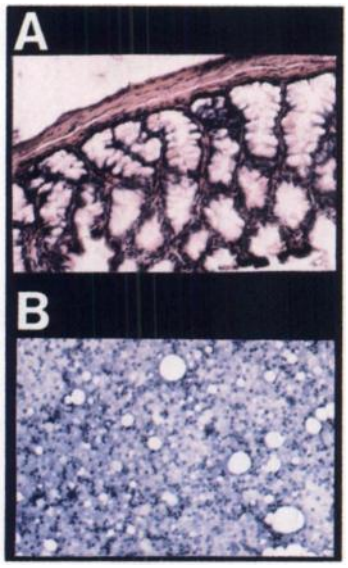

FIGURE 7. Autoradiographic images of thin (5–6 μm) sections of large intestine (A [× 600]; 2-mo exposure) and of bone marrow smears (B [× 600]; 4-mo exposure) of tumor-bearing rats following intravesical administration of [^{125}I]IUdR for 2 hr, showing absence of silver grains, i.e., no DNA-incorporated activity.

development [i.e., the hyperplasia stage (Fig. 6A) and the superficial disease stage of papillary carcinoma (Fig. 6B)], while the normal urothelium (Fig. 6D) was generally free of silver grains. In some tumor-bearing animals, labeling of a few seemingly normal urothelial cells was observed; the DNA incorporation by abnormal urothelium, however, was always significantly higher and control animals did not show uptake in the urothelium. Uptake was also observed in the basal layer of squamous metaplasia and in bacteria when active infection was present (these latter animals were excluded from the study). Animals with infection/inflammation demonstrated the potential for *IUdR to penetrate deep within the bladder wall since incorporation in inflammatory cells and newly formed capillary endothelial cells was seen deep within the stroma (Fig. 6C). Normal tissue sections developed serially over time (up to 4 mo of exposure) did not show the presence of silver grains associated with actively dividing normal epithelia, such as small (Fig. 7A) and large intestine (Fig. 7B). Of particular interest for therapeutic purposes, bone marrow smears (Fig. 7C) were also free of cell-associated silver grains indicating that stem cells did not incorporate *IUdR into their DNA.

DISCUSSION

5-Iodo-2′-deoxyuridine is a thymidine (TdR) analog that behaves remarkably like TdR, with efficient and specific incorporation into the DNA of dividing cells during the DNA synthetic (S) phase of the cell cycle (*16,17*). Most of the DNA-incorporated IUdR is retained for the life of the cell or its progeny (*18–21*). In contrast, unincorporated IUdR is rapidly catabolized and/or dehalogenated (*22,23*); its half-life in circulation is very short—less than 5 min in man and 7 min in mice (*20,22*). None of the major catabolic products are incorporated into nuclear DNA.

The Auger electron emitters ^{123}I and ^{125}I have been shown to be relatively innocuous when situated outside the nucleus (*24–26*), affixed to the cell membrane (*27*), or positioned extracellularly (*21,25,26*). On the other hand, when localized within the nucleus following DNA incorporation, *IUdR has demonstrated considerable toxicity in various normal and tumor mammalian cell lines in vitro (*21,24–31*) as well as therapeutic efficacy in vivo in a murine ovarian tumor (*7–9*), a rat brain

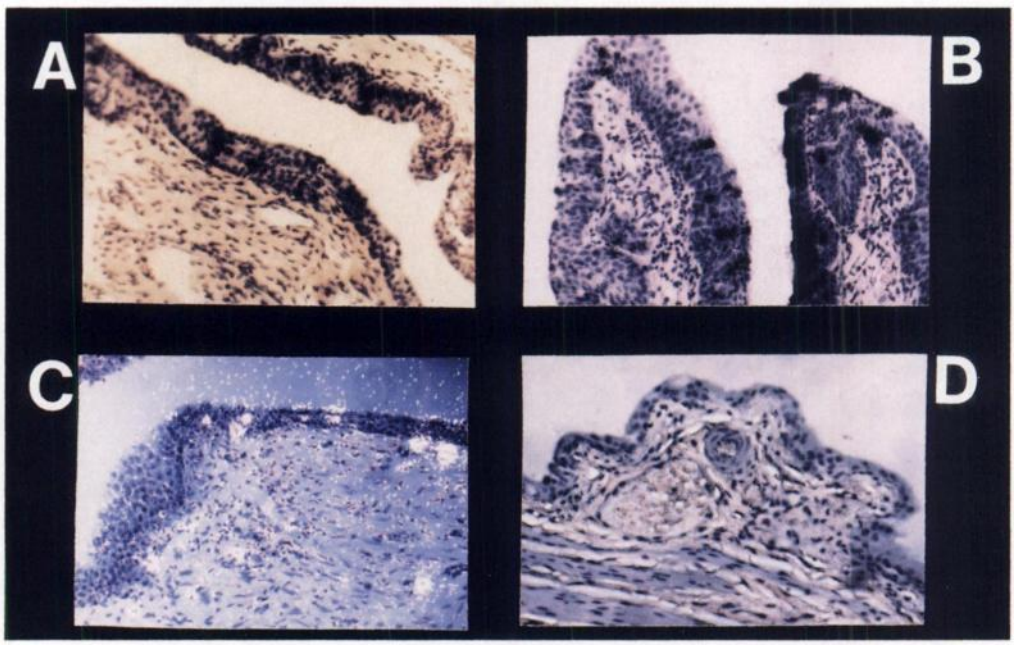

FIGURE 6. Autoradiographic images of thin (5–6 μm) sections obtained from bladders of tumor-bearing rats following intravesical administration of [^{125}I]IUdR for 2 hr show uptake in areas of hyperplasia (A [× 600]; 4-mo exposure) and papillary carcinoma (B [× 600]; 4-mo exposure) and in infection with inflammatory cells within stroma (C [× 600], dark field; 2-mo exposure). Normal urothelium (D [× 600]; 4-mo exposure) is free of silver grains.

tumor (*10*), and a rat intrathecal tumor (*11*) following its site-directed delivery. Our experience and that of others with this and several other Auger electron emitters have reiterated the dependence of Auger-electron-emitting toxicity on the intranuclear DNA localization of the radionuclide (*21,24–36*).

In addition to Auger electrons, ^{123}I also emits gamma rays suitable for gamma camera imaging. Since unincorporated IUdR is rapidly catabolized and eliminated (*22,23*), the resulting background activity is low, an ideal situation for imaging purposes. Furthermore, the high specific activity of this radionuclide (~8,500 TBq/mmole) will allow acquisition of images at early time points after administration, even when only a small amount of IUdR becomes incorporated. Experience with *IUdR in various animal [murine ovarian tumor (*9*), rat brain tumor (*12*)] and human [colon adenocarcinoma (*37*), bladder tumor (*38*)] cancers has confirmed that when *IUdR is delivered locoregionally, tumors can be visualized with optimal target-to-background ratios. Thus, the diagnostic potential of [^{123}I]IUdR in cancer can also be envisioned.

The clinical application of all therapeutic/diagnostic agents including IUdR requires high target-to-nontarget ratios for therapy as well as for imaging since normal tissues containing proliferating cells, such as the bone marrow or intestinal mucosa, are frequently dose-limiting. Because of its short half-life in circulation, the use of *IUdR requires tumors that are accessible to intralesional, intracavitary or intra-arterial administration to bypass the rapid and extensive dehalogenation and degradation, maximize uptake by the tumor and minimize the toxicity to normal dividing tissues.

Bladder cancer, which arises in the superficial lining of the urothelium and has a high frequency of recurrence (with macroscopic changes often absent despite positive cytology, as frequently occurs with carcinoma in situ), is a tumor for which direct delivery to the target can be implemented via intravesical administration of *IUdR. This route of administration provides a well controlled delivery system which not only prevents rapid systemic dispersal of the radiopharmaceutical, but also allows tumor cells to be exposed for appropriate time intervals to precise concentrations of *IUdR. This is a situation which is particularly desirable since *IUdR uptake is proportional to the exposure period as well as to its extracellular concentration (*21,26*). Finally, the well controlled delivery system and the low molecular weight will also aid in reducing instances of antibody responses to IUdR, thus facilitating repeated administration. Current therapy for carcinoma in situ and recurrent superficial papillary bladder tumors consists of intravesical administration of chemotherapeutic agents, such as bacillus Calmette-Guerin (BCG), thiotepa, mitomycin C and adriamycin (*39*). All of these agents carry the inherent risk of systemic illness and in some cases mortality (*40*). *IUdR offers a similar route of administration and the potential for far less adverse effects.

As outlined by Shaw and Mulshine (*41*), the evaluation of any new diagnostic or therapeutic cancer technique would require that, in addition to demonstrating high sensitivity and specificity, the uptake of the agent should: (a) reflect and be proportional to the state of differentiation and tumor burden, (b) be distinctive even in patients with small tumor volume and (c) reflect a change in the state or mass of tumor in response to therapy. Our results include several observations that fulfill these prerequisites and suggest the feasibility of diagnostic and/or therapeutic applications of *IUdR in human bladder cancer after intravesical administration. First, scintigraphic detection of bladder tumors was achieved with high sensitivity and specificity. Second, favorable tumor-to-normal tissue ratios were obtained. Third, *IUdR uptake was demonstrated at an early stage of tumor development (Ta or hyperplasia stage), while the radiopharmaceutical was not incorporated into the normal urothelium. Fourth, only a small fraction of the administered dose (<0.002%) appeared in the circulation in tumor-bearing rats and none of the normal dividing tissues, such as intestine or bone marrow, showed any *IUdR uptake. Finally, radiopharmaceutical uptake was observed in inflammatory cells and in neovasculature deep within the stroma demonstrating the ability of *IUdR to penetrate the bladder wall and therefore potentially target deep-seated cancer cells. It is also possible that following IUdR incorporation, such inflammatory cells may have migrated from more superficial layers to layers deeper within the bladder wall.

The ability to define the presence and degree of tumor aggressiveness permits one to assess the intrinsic biologic characteristics of the tumor, and thus allows prediction of the natural history of the disease on an individual basis by providing detection at an early stage, as well as identification of the patient population at increased risk of progression/recurrence. In addition, since these studies can be performed on the same patient over the course of his or her follow-up, longitudinal analysis can be conducted. Moreover, tailoring of the therapeutic regimen on an individual basis will become feasible.

CONCLUSION

We found that *IUdR injected intravesically was specifically incorporated into the DNA of tumor cells and not into that of the actively dividing epithelia of distant normal tissues examined or the bone marrow, resulting in high target-to-nontarget ratios. Additionally, after intravesical administration *IUdR uptake was observed at an early stage of tumor development deep within the bladder wall, suggesting that this radiopharmaceutical agent may therefore be useful for the diagnosis of tumor at various stages. As this tracer is selective for proliferating cells, it may also promote a better understanding of the intrinsic characteristics of the tumor and define its degree of aggressiveness as well as its response to various therapeutic modalities. Since DNA-incorporated, Auger-electron-emitting radionuclides have already been shown to be strongly antineoplastic, [^{123}I/^{125}I]IUdR could become an integral part of the therapeutic regimen of bladder cancer.

ACKNOWLEDGMENTS

Presented in part at the Second International Symposium on Biophysical Aspects of Auger Processes, July 1991; the Fortieth Annual Meeting of the Radiation Research Society, March 1992; and the Fortieth Annual Meeting of the Society of Nuclear Medicine, June 1993. Supported by National Institutes of Health grant RO1 CA 15523.

REFERENCES

1. Kantoff PW, Shipley WU, Gallagher J, Loughlin KR, Soto EA. Cancer of the bladder. In: Osteen RT, ed. *Cancer manual*, 8th ed. Boston: American Cancer Society; 1990:295–303.
2. Boring CC, Squires TS, Tong T. Cancer statistics 1993. *CA Cancer J Clin* 1993;43: 7–26.
3. Raghavan D, Shipley WU, Garnick MB, Russell PJ, Richie JP. Biology and management of bladder cancer. *N Engl J Med* 1990;322:1129–1138.
4. Whitmore WF Jr. Bladder cancer: an overview. *CA Cancer J Clin* 1988;38:213–223.
5. Boileau MA, Swartz D, Schmidt KL, Schmidt WA. Limitations of flow cytometric DNA analysis for the diagnosis of bladder cancer. *J Surg Oncol* 1989;40:194–200.
6. Williams NN, Daly JM. Flow cytometry and prognostic implications in patients with solid tumors. *Surg Gynecol Obstet* 1990;171:257–266.
7. Bloomer WD, Adelstein SJ. Antineoplastic effect of iodine-125-labeled iododeoxyuridine. *Int J Radiat Biol* 1975;27:509–511.
8. Bloomer WD, Adelstein SJ. 5-^{125}I-iododeoxyuridine as prototype for radionuclide therapy with Auger emitters. *Nature* 1977;265:620–621.
9. Baranowska-Kortylewicz J, Makrigiorgos GM, Van den Abbeele AD, Berman RM, Adelstein SJ, Kassis AI. 5[^{123}I]iodo-2′-deoxyuridine in the radiotherapy of an early ascites tumor model. *Int J Radiat Oncol Biol Phys* 1991;21:1541–1551.

10. Kassis AI. Toxicity and therapeutic effects of low-energy electrons. *Nucl Instrum Meth Phys Res [B]* 1994;87:279–284.
11. Kassis AI, Adelstein SJ. Preclinical animal studies with radiolabeled IUdR. *J Nucl Med* 1996;37:343–352.
12. Kassis AI, Van den Abbeele AD, Wen PYC, et al. Specific uptake of the Auger electron-emitting thymidine analogue 5-[^{123}I/^{125}I]iodo-2′-deoxyuridine in rat brain tumors: diagnostic and therapeutic implications in humans. *Cancer Res* 1990;50:5199–5203.
13. Sufrin G, Meyer JS, Martin SA, Schechtman K. Proliferative activity of urothelium and tumors of renal pelvis, ureter, and urinary bladder evaluated by thymidine labeling. *Urology* 1984;23(suppl):15–22.
14. Hicks RM, Wakefield JSJ. Rapid induction of bladder cancer in rats with N-methyl-N-nitrosourea. I. Histology. *Chem Biol Interact* 1972;5:139–152.
15. Baranowska-Kortylewicz J, Kinsey BM, Layne WW, Kassis AI. Radioiodo-demercuration: a simple synthesis of 5-[$^{123/125/127}$I]iodo-2′-deoxyuridine. *Appl Radiat Isot* 1988;39:335–341.
16. Eidinoff ML, Cheong L, Rich MA. Incorporation of unnatural pyrimidine bases into deoxyribonucleic acid of mammalian cells. *Science* 1959;129:1550–1551.
17. Morris NR, Cramer JW. DNA synthesis by mammalian cells inhibited in culture by 5-iodo-2′-deoxyuridine. *Mol Pharmacol* 1966;2:1–9.
18. Calabresi P, Cardoso SS, Finch SC, et al. Initial clinical studies with 5-iodo-2′-deoxyuridine. *Cancer Res* 1961;21:550–559.
19. Hughes WL, Commerford SL, Gitlin D, et al. Deoxyribonucleic acid metabolism in vivo. I. Cell proliferation and death as measured by incorporation and elimination of iododeoxyuridine. *Fed Proc* 1964;23:640–648.
20. Commerford SL. Biological stability of IUdR labeled with ^{125}I after incorporation into the DNA of the mouse. *Nature (London)* 1965;206:949–950.
21. Kassis AI, Sastry KSR, Adelstein SJ. Kinetics of uptake, retention and radiotoxicity of ^{125}IUdR in mammalian cells: implications of localized energy deposition by Auger processes. *Radiat Res* 1987;109:78–89.
22. Prusoff WH. A review of some aspects of 5-^{125}I-iododeoxyuridine and azauridine. *Cancer Res* 1963;23:1246–1259.
23. Klecher RW Jr, Jenkins JF, Kinsella TJ, Fine RL, Strong JM, Collins JM. Clinical pharmacology of 5-iodo-2′-deoxyuridine and 5-iodouracil and endogenous pyrimidine modulation. *Clin Pharmacol Ther* 1985;38:45–51.
24. Hofer KG, Harris CR, Smith JM. Radiotoxicity of intracellular ^{67}Ga, ^{125}I and ^{3}H: nuclear versus cytoplasmic radiation effects in murine L1210 leukaemia. *Int J Radiat Biol* 1975;28:225–241.
25. Kassis AI, Fayad F, Kinsey BM, Sastry KSR, Taube RA, Adelstein SJ. Radiotoxicity of ^{125}I in mammalian cells. *Radiat Res* 1987;111:305–318.
26. Makrigiorgos GM, Kassis AI, Baranowska-Kortylewicz J, et al. Radiotoxicity of 5-[^{123}I]iodo-2′-deoxyuridine in V79 cells: a comparison with 5-[^{125}I]iodo-2′-deoxyuridine. *Radiat Res* 1989;118:532–544.
27. Warters RL, Hofer KG, Harris CR, Smith JM. Radionuclide toxicity in cultured mammalian cells: elucidation of the primary site of radiation damage. *Curr Top Radiat Res Q* 1977;12:389–407.
28. Hofer KG, Hughes WL. Radiotoxicity of intranuclear tritium, ^{125}iodine and ^{131}iodine. *Radiat Res* 1971;47:94–109.
29. Bradley EW, Chan PC, Adelstein SJ. The radiotoxicity of iodine-125 in mammalian cells I. Effects on the survival curve of radioiodine incorporated into DNA. *Radiat Res* 1975;64:555–563.
30. Chan PC, Lisco E, Lisco H, Adelstein SJ. The radiotoxicity of iodine-125 in mammalian cells II. A comparative study on cell survival and cytogenetic responses to ^{125}IUdR, ^{131}IUdR and ^{3}HTdR. *Radiat Res* 1976;67:332–343.
31. Sundell-Bergman S, Johanson KJ. Repairable and unrepairable DNA strand breaks induced by decay of ^{3}H and ^{125}I incorporated into DNA of mammalian cells. *Radiat Environ Biophys* 1980;18:239–248.
32. Kassis AI, Adelstein SJ, Haydock C, Sastry KSR. Radiotoxicity of ^{75}Se and ^{35}S: theory and application to a cellular model. *Radiat Res* 1980;84:407–425.
33. Kassis AI, Adelstein SJ, Haydock C, Sastry KSR, McElvany KD, Welch MJ. Lethality of Auger electrons from the decay of bromine-77 in the DNA of mammalian cells. *Radiat Res* 1982;90:362–373.
34. Kassis AI, Adelstein SJ, Haydock C, Sastry KSR. Thallium-201: an experimental and a theoretical radiobiological approach to dosimetry. *J Nucl Med* 1983;24:1164–1175.
35. Kassis AI, Sastry KSR, Adelstein SJ. Intracellular distribution and radiotoxicity of chromium-51 in mammalian cells: Auger-electron dosimetry. *J Nucl Med* 1985;26:59–67.
36. Kassis AI, Howell RW, Sastry KSR, Adelstein SJ. Positional effects of Auger decays in mammalian cells in culture. In: Baverstock KF, Charlton DE, eds. *DNA damage by Auger emitters*. London: Taylor & Francis, Ltd.; 1988:1–13.
37. Mariani G, Di Sacco S, Volterrani D, et al. Intra-arterial infusion of 5-[^{123}I]iodo-2′-deoxyuridine in patients with inoperable liver metastases from colorectal cancer. In: *Program and Abstracts of the Forty-second Annual Meeting of the Radiation Research Society*, Nashville, TN; April 29–May 4, 1994:208.
38. Harrison K, Dalrymple GV, Baranowska-Kortylewicz J. Bladder cancer-[123I]IUdR imaging in preparation for [125I]IUdR therapy [Abstract]. *J Nucl Med* 1994;35:144P.
39. Herr HW, Laudone VP, Whitmore WF, Jr. An overview of intravesical therapy for superficial bladder tumors. *J Urol* 1987;138:1363–1368.
40. Catalona WJ, Hudson MA, Gillen DP, Andriole GL, Ratliff TL. Risks and benefits of repeated courses of intravesical bacillus Calmette-Guerin therapy for superficial bladder cancer. *J Urol* 1987;137:220–224.
41. Shaw GL, Mulshine JL. Biomarkers in early detection of lung cancer. *Contemp Oncol* July/August 1991;43–51.

Feasibility of Fluorine-18-Fluorophenylalanine for Tumor Imaging Compared with Carbon-11-L-Methionine

Kazuo Kubota, Kiichi Ishiwata, Roko Kubota, Susumu Yamada, Jutaro Takahashi, Yoshinao Abe, Hiroshi Fukuda and Tatsuo Ido

Department of Nuclear Medicine and Radiology, Institute of Development, Aging and Cancer and Cyclotron and Radioisotope Center, Tohoku University, Sendai, Japan; and Tokyo Metropolitan Institute for Gerontology, Tokyo, Japan

L-[methyl-^{11}C]methionine (^{11}C-Met) is a useful tracer for tumor imaging with PET. The drawbacks include a short half-life and high physiological accumulation in abdominal organs. To overcome these shortfalls, the feasible use of [^{18}F]fluorophenylalanine (^{18}F-Phe), which shares the same amino acid transport system with Met, for tumor imaging was examined. **Methods:** The time course of tissue distribution of ^{18}F-Phe and the tumor uptake response to radiotherapy were compared with ^{14}C-Met and [^{3}H] thymidine (^{3}H-Thd) in the rat AH109A tumor model. Intratumoral distribution of ^{18}F-Phe was compared with ^{14}C-Met and ^{14}C-Thd using double-tracer macroautoradiography (ARG). We also evaluated whole-body ARG. **Results:** Tumor uptake of ^{18}F-Phe peaked at 60 min postinjection and was higher than that of the liver, intestine and kidney but lower than the pancreas. Tumor uptake of ^{18}F-Phe was similar to that of ^{14}C-Met. Tumor-to-blood and tumor-to-muscle ratios were higher in ^{14}C-Met compared with that of ^{18}F-Phe because of the rapid blood clearance of ^{14}C-Met. With whole-body ARG, the tumor was clearly visualized with high contrast. Radiotherapeutic response of tumor uptake of ^{18}F-Phe was as rapid as that with ^{14}C-Met and with ^{3}H-Thd. Intratumoral distribution of ^{18}F-Phe and ^{14}C-Met were identical, and ^{18}F-Phe and ^{14}C-Thd were similar. **Conclusion:** Fluorine-18-Phe seems to be a potentially useful amino acid tracer for tumor imaging with a longer half-life than ^{11}C, with higher tumor contrast in the abdomen than Met and a similar sensitive response to radiotherapy.

Key Words: fluorine-18-fluorophenylalanine; autoradiography; carbon-11-methionine; PET; fluorine-18-FDG

J Nucl Med 1996; 37:320–325

A glucose analog, ^{18}F-2-fluoro-2-deoxy-D-glucose (FDG), and an essential amino acid tracer, L-[methyl-^{11}C]methionine (^{11}C-Met), have been used for tumor imaging with PET. Carbon-11-Met is useful for the diagnosis of the brain (*1*), head

Received Dec. 27, 1994; revision accepted Jun. 7, 1995.

For correspondence or reprints contact: Kazuo Kubota, MD, Department of Nuclear Medicine and Radiology, Institute of Development, Aging and Cancer, Tohoku University, 4-1 Seiryomachi, Aoba-ku, Sendai 980-77, Japan.